

# Classification of precipitation events with a convective response timescale and their forecasting characteristics

M. Zimmer,<sup>1</sup> G. C. Craig,<sup>2</sup> C. Keil,<sup>2</sup> and H. Wernli<sup>3</sup>

Received 15 November 2010; revised 17 January 2011; accepted 28 January 2011; published 1 March 2011.

[1] The convective timescale  $\tau_c$ , which is mainly determined by the ratio of CAPE and precipitation rate, provides a physically-based measure to distinguish equilibrium and non-equilibrium convection. A statistical analysis of this timescale, based upon observational data from radiosonde ascents, rain gauges, and radar for seven warm seasons in Germany, reveals that the equilibrium and non-equilibrium regimes can be regarded as extremes of a continuous distribution. The two regimes characterize very different interactions between the large-scale flow and convection. The quality of precipitation forecasts from a non-hydrostatic regional weather prediction model with parameterized convection differs substantially for the two regimes, with strong overestimations and too large precipitation objects for the non-equilibrium events. **Citation:** Zimmer, M., G. C. Craig, C. Keil, and H. Wernli (2011), Classification of precipitation events with a convective response timescale and their forecasting characteristics, *Geophys. Res. Lett.*, 38, L05802, doi:10.1029/2010GL046199.

## 1. Introduction

[2] Many properties of cumulus convection, including its predictability, depend on the large-scale (synoptic and mesoscale) environment in which it is embedded. To some degree the convective activity can be regarded as under the control of the larger scales, and indeed this is the basis of most cumulus parameterisation schemes in numerical models, but this control is only partial, and the degree of control is likely to vary with time and place [see, e.g., Arakawa, 2004].

[3] The initiation and lifecycle of a convective cloud is directly a result of processes local to the cloud itself: the conditional instability of the column, the absence of a capping inversion or other inhibiting factors, and the boundary layer variability that can trigger an updraft. If these factors are present a cloud will rapidly form, developing within about a half hour.

[4] Conversely there are two ways in which convection can be prevented. First, in the absence of processes such as large-scale ascent that cools the troposphere and creates conditional instability, the Convective Available Potential Energy (CAPE) may be rapidly exhausted. Second, if the triggering processes in the boundary layer are not strong enough to

overcome the energy barrier of Convective Inhibition (CIN), convection will not occur even in the presence of large CAPE. Either of these processes may control convection, leading to two scenarios for the influence of large scales on convection. If convection is limited by the availability of CAPE, the amount of convection (mass flux, precipitation etc.) will be controlled by the rate at which the larger scale flow creates new CAPE. Since individual clouds still respond to local influences, only the average amount of convection is constrained, leading to a statistical equilibrium (also called quasi-equilibrium or in this paper simply equilibrium). If, on the other hand, the amount of convection is limited by the interaction of triggering processes with CIN, large amounts of CAPE may build up, and there is no reason to expect a close relationship between the amount of convection and the large-scale flow.

[5] The two regimes, *equilibrium* and *triggered convection*, represent dramatically different modes of interaction between the convection and larger scales, and it would be desirable to be able to distinguish which is dominant in a given meteorological situation. One possibility would be to look at CAPE, which would be expected to be small in equilibrium situations [Emanuel *et al.*, 1994]. However the amount of CAPE is variable, even in equilibrium, and it is impossible to identify a threshold value that distinguishes the two regimes. A more fundamental approach, introduced by Arakawa and Schubert [1974] would be to compare the rate at which conditional instability is created by the large-scale flow with the rate at which it is destroyed by convection. The synoptic scale flow evolves on a timescale of a day or so, while in the absence of inhibiting factors, convection could be expected to remove CAPE with a turnover time of about an hour. If this is the case, the rate of convection will closely follow the large-scale forcing. On the other hand, a longer convective timescale would indicate that the convection is not constrained by the forcing and equilibrium is not present.

[6] In this work, we will estimate the timescale for removal of conditional instability by convection,  $\tau_c$ , defined schematically as

$$\tau_c \sim \frac{CAPE}{dCAPE/dt},$$

where CAPE is given by

$$CAPE = \int \frac{g}{T_0} (T_a - T) dz,$$

with  $T$  the environmental temperature,  $T_a$  the temperature of a pseudo-adiabatically lifted boundary layer parcel, and  $T_0$  a constant reference temperature.

[7] Following Done *et al.* [2006], we note that the CAPE can be removed by supplying enough heat to eliminate the

<sup>1</sup>Institute for Atmospheric Physics, University of Mainz, Mainz, Germany.

<sup>2</sup>Meteorologisches Institut, Ludwigs-Maximilians Universität, Munich, Germany.

<sup>3</sup>Institute for Atmospheric and Climate Science, ETH Zurich, Zurich, Switzerland.

difference between  $T$  and  $T_a$  through the column. The vertically integrated latent heat release can be determined from the precipitation rate  $P$  ( $\text{kg s}^{-1} \text{m}^{-2}$ )

$$L_v P = \int \rho C_p \frac{dT}{dt} dz,$$

so that

$$\frac{d\text{CAPE}}{dt} = \frac{L_v}{C_p} \frac{g}{\rho T_o} P.$$

[8] The convective timescale can then be estimated as

$$\tau_c = \frac{1}{2} \frac{C_p}{L_v} \frac{\rho T_o}{g} \frac{\text{CAPE}}{P}.$$

The factor of 1/2 is introduced because this calculation ignores convective modification of the boundary layer, and will thus over-estimate the convective timescale significantly. The value of 1/2 corresponds to the assumption that tropospheric heating and boundary cooling (and drying) contribute equally to the reduction of CAPE [e.g., *Betts*, 1986].

[9] The equilibrium limit occurs when  $\tau_c$  is short in comparison with the time over which the large-scale flow evolves and creates CAPE, ranging from 24 hrs (diurnal cycle) to several days (synoptic cyclone). In the radiative-convective equilibrium simulations of *Cohen and Craig* [2004], convection responded to changes in large-scale forcing on a time-scale of about an hour, but the value depended on the large scale forcing. Triggered convection occurs in the limit of large values of the convective timescale. In the case considered by *Done et al.* [2006], values of tens or hundreds of hours were found, with a tendency to decrease systematically through the duration of the event as precipitation increased and CAPE decreased once convection was initiated. Indeed, a transition to equilibrium is possible, with values of  $\tau_c$  not corresponding to either extreme.

[10] Previous studies have sometimes found it useful to define a threshold to distinguish the equilibrium regime (controlled by the large scales), from the remaining non-equilibrium events (triggered convection and transitional events). *Keil and Craig* [2011] examined forecast uncertainty of convective precipitation of a convection-permitting ensemble prediction system and identified a weather regime dependence. *Molini et al.* [2011] found that large or small values of  $\tau_c$ , corresponding to equilibrium or non-equilibrium convection, correlate to changes in the morphology of observed precipitation events. An arbitrary threshold value of 6 hours was used in these studies, but given the uncertainties in estimating both  $\tau_c$  and the timescale of the large-scale processes, only order of magnitude differences in  $\tau_c$  should be regarded as significant. On the other hand G. C. Craig et al. (Constraints on the impact of radar rainfall data assimilation on forecasts of cumulus convection, submitted to *Quarterly Journal of the Royal Meteorological Society*, 2011) showed that the length of time that a high resolution model retains information from assimilation of radar reflectivity is proportional to  $\tau_c$  over values ranging from 0.5 to 100 hours.

[11] Each of the studies cited above relied on model or reanalysis data for the calculation of  $\tau_c$ . The first aim of this

paper is to present calculations of  $\tau_c$  based purely on observational data, and thus provide a first estimate for the relative frequency of equilibrium and non-equilibrium convection in nature. This will be done using a multi-year data set of summertime radiosonde ascents over Germany, combined with a high-resolution precipitation data set. The second goal of the paper is to demonstrate the utility for verification of numerical models of considering equilibrium and non-equilibrium events separately, by showing that for a particular numerical model the error characteristics are quite different in the two regimes.

## 2. Data and Methods

### 2.1. Radiosonde Data

[12] For this study, a seven year period (2001–2007, May–October) from seven radiosonde stations in Germany, namely (from north to south) Bergen (WMO-No. 10238, 9.93°E, 52.82°N, 77 m above sea level), Lindenberg (10393, 14.12°E, 52.22°N, 115 m), Essen (10410, 6.97°E, 51.40°N, 153 m), Meiningen (10548, 10.38°E, 50.57°N, 453 m), Idar Oberstein (10618, 7.33°E, 49.70°N, 377 m), Stuttgart (10739, 9.20°E, 48.83°N, 315 m), and Oberschleissheim (10868, 11.55°E, 48.25°N, 489 m) is examined. Up to four radiosonde observations per day (at 00, 06, 12, and 18 UTC) are available. The data were obtained from the University of Wyoming (<http://weather.uwyo.edu/upperair/sounding.html>).

### 2.2. CAPE

[13] CAPE is calculated from the radiosonde observations, with the assumption of a pseudo-adiabatic lifted boundary layer air parcel, and considering only the liquid phase. Initial values for the hypothetical air parcel (temperature and humidity) are obtained by averaging over the lowest 100 hPa of the radiosonde profile. The computation of the vertical profile is performed by using the routines introduced by *Früh and Wirth* [2007].

### 2.3. Precipitation Observations

[14] The precipitation data were obtained from a high-resolution data set over Germany [*Paulat et al.*, 2008] that combines rain gauge and radar information. Hourly precipitation sums with a mesh size of 7 km are accumulated over three hours within a circle (radius equal 50 km) centered on the radiosonde times and locations. For the determination of  $\tau_c$ , precipitation sums are transformed to precipitation rates.

### 2.4. Model Description

[15] The model data are taken from the Swiss version of the non-hydrostatic model of the COSMO consortium ([www.cosmo-model.org](http://www.cosmo-model.org)) and is the counterpart of the former German “Lokalmodell”, described by *Steppeler et al.* [2003]. The horizontal grid spacing is 7 km and moist convection is treated by the mass flux convergence scheme of *Tiedtke* [1989]. In this study, three hourly precipitation accumulations were analyzed within the same circular regions around the radiosonde locations as for the observations. The investigations have been confined to operational forecasts of COSMO-7 initialized at 00 UTC.

### 2.5. The SAL Technique

[16] The feature-based quality measure SAL [*Wernli et al.*, 2008, 2009] was developed to investigate the performance of

**Table 1.** Total Number of Cases and Percentage Where  $\tau_c$  is Below a Certain Threshold Value, for the Entire Warm Season (MJJASO) and Separately for the Months JJA and MSO

$\tau$ [hrs]	n	<1	<3	<6	<12	<24
MJJASO, [%]	n = 4790	35.3	48.5	55.8	62.5	69.1
JJA, [%]	n = 3264	31.2	44.9	52.0	59.0	66.6
MSO, [%]	n = 1526	44.1	56.2	64.1	69.9	74.6

Quantitative Precipitation Forecasts (QPFs). SAL contains three independent components measuring the quality of the (S)tructure, (A)mplitude and (L)ocation of the QPFs. The values for  $S$  and  $A$  are within  $[-2, +2]$  and for  $L$  within  $[0, +2]$ , where 0 denotes the perfect score for all three components. This verification measure will be used in the second part of the study to assess the quality of COSMO-7 model QPFs for different regimes of  $\tau_c$ .

### 3. Results

#### 3.1. Climatology of Convective Timescale

[17] The first question to be addressed is the relative frequency of equilibrium convection, where large-scale creation of instability is the controlling factor. As discussed in the introduction, this is expected to be the case when the convective timescale is shorter than about 6 hrs. Since this value is rather arbitrary, Table 1 shows the fraction of events with  $\tau_c$  smaller than several choices of threshold value. Almost 50% of convective events have  $\tau_c$  less than 3 hours, 56% have values less than 6 hours, and 63% less than 12 hours, indicating that more than half of warm season convective events are equilibrium. These values are slightly lower for the summer months JJA. Not included in Table 1 are the 5140 radiosonde times where precipitation occurred, but the convective timescale was zero. This occurs when CAPE is zero, and the precipitation is presumably non-convective.

[18] Figure 1 shows the frequency of occurrence of values of  $\tau_c$  for the complete data set, separated into summer (June, July, August) and transitional season months (May, September, October). The distributions closely follow a power law with exponents around  $-1.3$ . There is no clear distinction between equilibrium and non-equilibrium regimes, although there is some suggestion of a scale break, with shallower slope for  $\tau_c$  smaller than about 10 hours and steeper slope for large  $\tau_c$ . A sharp transition would not be expected since many different meteorological environments with different synoptic timescales have been combined. It is also interesting to speculate that regions of large and small  $\tau_c$  are intermixed within the spatial averaging area, as would be expected near the critical point of a phase transition [Peters and Neelin, 2006]. In this case the  $\tau_c$  value would reflect which of the two phases is dominant.

[19] Comparing the two curves in Figure 1 for the summer and transitional seasons shows that the slope for the summer months is shallower, corresponding to proportionally more events with long convective timescales and thus more non-equilibrium convection. Frequency distributions of  $\tau_c$  were also prepared for each station individually, and for different times of day, but none were significantly different from Figure 1.

[20] Since the convective timescale is determined by the ratio of CAPE and precipitation rate it is interesting to consider how the two factors contribute. Scatter plots of  $\tau_c$  against precipitation and CAPE both show significant correlation, indicating that both contribute to the variation in timescale (not shown). On the other hand precipitation and CAPE are not correlated with each other, showing that each is contributing independent information to the result.

#### 3.2. Evaluation of COSMO-7 Model

[21] As an example for the application of the convective timescale concept, QPFs from the COSMO-7 model have been verified at 12 UTC for summer (JJA) rainfall. For the

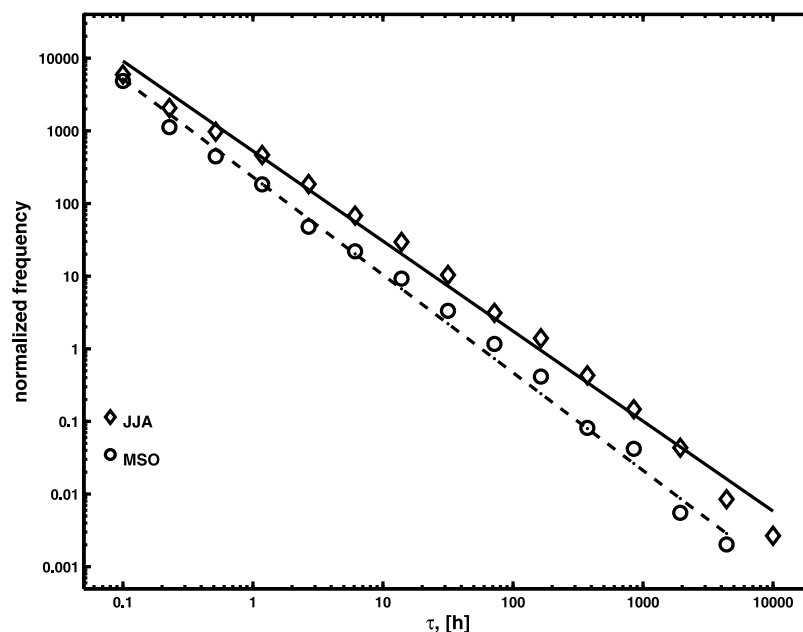


**Figure 1.** Loglog diagram of frequency of  $\tau_c$  for summer (JJA) in diamonds and for May, September and October (MSO) as open circles. The regression line for summer (solid line) has a slope of  $-1.24$  and for MSO (dash-dotted) of  $-1.35$ .

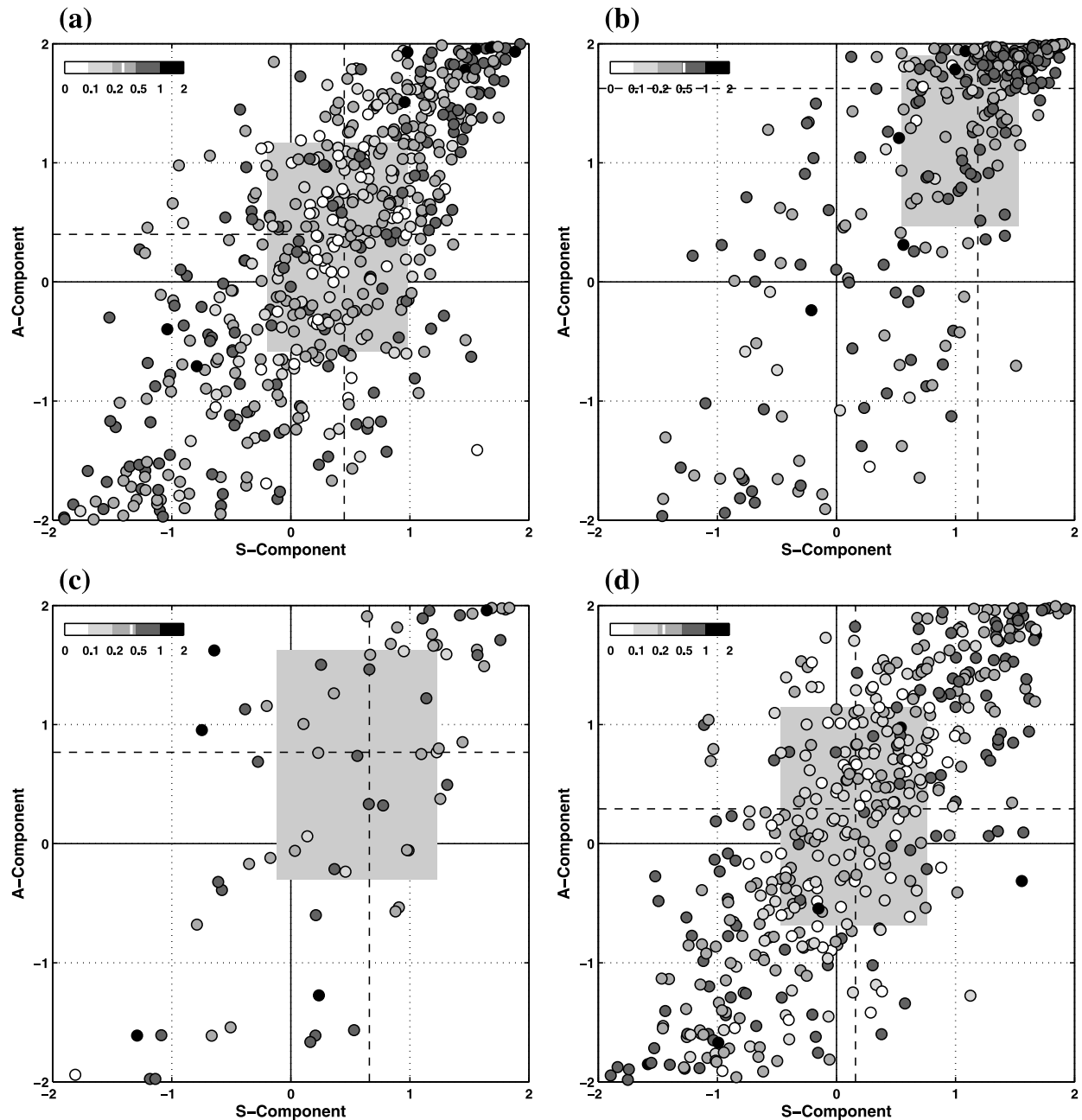


**Figure 2.** SAL diagrams for 3-hourly accumulated QPFs from COSMO-7 during summer (JJA) centered at 12 UTC for three weather regimes: (a) low  $\tau_c$  ( $\leq 12$  h), (b) high  $\tau_c$  ( $> 12$  h), and (d) CAPE = 0 for all stations except Stuttgart. (c) The results for  $\tau_c > 12$  h for Stuttgart. Dashed lines indicate the median values of  $S$  and  $A$ , and gray-shaded boxes denote the intersection of the 25th and 75th percentiles of both components.  $L$  values are indicated by the color of the dots (see grayscale in top left, with the median of  $L$  shown by the white line).

QPF verification, the feature-based technique SAL has been used and the data set has been divided into two classes by using  $\tau_c = 12$  h as a threshold (similar results are obtained with a 6 h threshold). The first class contains situations with a short convective response time ( $\tau_c \leq 12$  h) and the second class above this threshold. The number of events within the first class is approximately twice that of the second class.

[22] Figures 2a and 2b show SAL diagrams [Wernli et al., 2008] of the two classes for all stations except Stuttgart. The

results for high  $\tau_c$  conditions at Stuttgart are shown separately in Figure 2c. Additionally, the situations where CAPE equals zero are depicted in Figure 2d for all stations except Stuttgart.

[23] For the short convective response time category (Figure 2a), most of the points are found in the top right and bottom left quadrant of the diagram. Many entries are along the main diagonal showing that the model tends to overestimate the amount of precipitation in the region by producing too large and/or flat precipitation objects (positive values of

$A$  and  $S$ ). Analogously, underestimated amounts are accompanied by too small and/or peaked objects (negative values of  $A$  and  $S$ ). The median values of  $S$  and  $A$  are slightly positive (both about 0.4). The relatively large values of the interquartile range (about 1.8 for  $A$  and 1.2 for  $S$ ) indicate that the QPFs frequently score poorly in one or both of the two components. In contrast, the QPF performance of COSMO-7 for the high  $\tau_c$ -values (Figure 2b) is dramatically different. Most of the forecasts are characterized by positive values of  $S$  and  $A$ , as evidenced by the high median values for  $S$  (1.2) and  $A$  (1.6), showing the model with parameterised convection tends to overestimate precipitation by producing oversized, overly homogeneous rain regions. Also the median of  $L$  is clearly worse for the high  $\tau_c$ -values, indicating pronounced errors in the location of the precipitation events.

[24] A special case is Stuttgart (Figure 2c), where the separation between the two regimes is not as dramatic as for the other stations. The median values for  $S$  (0.7) and  $A$  (0.8) for Stuttgart are considerably lower for the high  $\tau_c$  cases, but higher for the low  $\tau_c$  cases when compared to the median values of all other stations. It may be that the hilly topography near Stuttgart (compared to other stations) leads to greater variability in the forecast precipitation fields. The presumably non-convective precipitation events, where CAPE is zero (Figure 2d), have also been investigated. The results are similar to the case with low  $\tau_c$  values, having slightly smaller median values for  $S$  (0.2),  $A$  (0.3), and  $L$ .

#### 4. Conclusions

[25] The convective timescale  $\tau_c$ , which is mainly determined by the ratio of CAPE and precipitation rate, provides a physically meaningful distinction between equilibrium and non-equilibrium convection that occurs in the spatial and temporal vicinity of a radiosonde (50 km and  $\pm 1.5$  hr, respectively). The two regimes, characterized by small and large values of  $\tau_c$ , respectively, correspond to different mechanisms of interaction between the large-scale flow (leading to the build-up of CAPE) and convection (leading to the destruction of CAPE). For the first time,  $\tau_c$  has been statistically assessed using observational data only (CAPE from radiosonde ascents, precipitation from a combined gauge-radar product) for a time period of 7 warm seasons and at 7 radiosonde stations in Germany. The results show that the equilibrium and non-equilibrium regimes constitute extremes of a continuous distribution that does not show a clear break in the histogram. If considering a threshold of 12 hours to separate the two categories, there is about a ratio of 2:1 between the number of events with equilibrium and non-equilibrium convection in the considered region and time period.

[26] In addition to providing a statistics of observation-based values of  $\tau_c$ , the quality of QPFs of the non-hydrostatic operational mesoscale numerical weather prediction model COSMO-7 has been evaluated with the feature-based verification technique SAL. The analysis reveals a scattered behavior for the equilibrium cases (reasonable quality on average) and large systematic errors for the non-equilibrium situations (strong overestimation and too large precipitation objects).

[27] The main caveats of this study are associated with the use of a particular definition of CAPE to estimate the

convective timescale, the use of precipitation to estimate the rate of removal of CAPE by convection, and the geographical representativity of this study. CAPE values are sensitive to assumptions about the treatment of hydrometeors and the initial conditions used for the air parcel ascent. Processes other than latent heat release associated with precipitation have been considered only through a crude correction factor. Although different assumptions would lead to different absolute values, they would not likely result in the order of magnitude changes to  $\tau_c$  that would be required to change the position of a particular meteorological situation within the overall distribution. The third caveat is related to the consideration of locations within Germany only. It would be worthwhile to perform similar investigations in other regions (e.g., with differing topography, land-sea contrast, and radiative forcing) to assess the generality of the statistical distribution of  $\tau_c$ . Also, it will be important to assess the quality of QPFs from other models and in other geographical areas for the two contrasting types of convection.

[28] **Acknowledgments.** We thank Martin Göber and two anonymous referees for their constructive comments. We are very grateful to Barbara Früh, Ralf Faßnacht, and Marcus Paulat for their earlier work on CAPE calculations in Germany and for their technical help. We thank the German Weather Service, Meteo Swiss, and the University of Wyoming for providing the rain gauge and radar observations, COSMO-7 forecasts, and radiosonde data, respectively. MZ acknowledges funding from the German Research Foundation (DFG) priority program on Quantitative Precipitation Forecasts (SPP 1167).

#### References

- Arakawa, A. (2004), The cumulus parameterization problem: Past, present, and future, *J. Clim.*, *17*, 2493–2525.
- Arakawa, A., and W. H. Schubert (1974), Interaction of a cumulus cloud ensemble with the large-scale environment. Part I, *J. Atmos. Sci.*, *31*, 674–701.
- Betts, A. K. (1986), A new convective adjustment scheme. Part I: Observational and theoretical basis, *Q. J. R. Meteorol. Soc.*, *112*, 677–691.
- Cohen, B. G., and G. C. Craig (2004), The response time of a convective cloud ensemble to a change in forcing, *Q. J. R. Meteorol. Soc.*, *130*, 933–944.
- Done, J. M., G. C. Craig, S. L. Gray, P. A. Clark, and M. E. B. Gray (2006), Mesoscale simulations of organised convection: Importance of convective-equilibrium, *Q. J. R. Meteorol. Soc.*, *132*, 737–756.
- Emanuel, K. A., J. D. Neelin, and C. S. Bretherton (1994), On large-scale circulations in convecting atmospheres, *Q. J. R. Meteorol. Soc.*, *120*, 1111–1143.
- Früh, B., and V. Wirth (2007), Convective Available Potential Energy (CAPE) in mixed phase cloud conditions, *Q. J. R. Meteorol. Soc.*, *133*, 561–569.
- Keil, C., and G. C. Craig (2011), Regime-dependent forecast uncertainty of convective precipitation, *Meteorol. Z.*, in press.
- Molini, L., A. Parodi, N. Reboraa, and G. C. Craig (2011), Classifying severe rainfall events over Italy by hydrometeorological and dynamical criteria, *Q. J. R. Meteorol. Soc.*, *137*, 148–154.
- Paulat, M., C. Frei, M. Hagen, and H. Wernli (2008), A gridded dataset of hourly precipitation in Germany: Its construction, climatology and application, *Meteorol. Z.*, *17*, 719–732.
- Peters, O., and J. D. Neelin (2006), Critical phenomena in atmospheric precipitation, *Nat. Phys.*, *2*, 393–396, doi:10.1038/nphys314.
- Stappeler, J., G. Doms, U. Schättler, H. W. Bitzer, A. Gassmann, U. Damrath, and G. Gregoric (2003), Meso-gamma scale forecasts using the nonhydrostatic model LM, *Meteorol. Atmos. Phys.*, *82*, 75–96.
- Tiedtke, M. (1989), A comprehensive mass flux scheme for cumulus parameterization in large scale models, *Mon. Weather Rev.*, *117*, 1779–1799.
- Wernli, H., M. Paulat, M. Hagen, and C. Frei (2008), SAL—A novel quality measure for the verification of quantitative precipitation forecasts, *Mon. Weather Rev.*, *136*, 4470–4487.

Wernli, H., C. Hofmann, and M. Zimmer (2009), Spatial forecast verification methods intercomparison project: Application of the SAL technique, *Weather Forecast.*, 24, 1472–1484.

---

G. C. Craig and C. Keil, Meteorologisches Institut, Ludwigs-Maximilians Universität, Theresienstrasse 37, D-80333 München, Germany.

H. Wernli, Institute for Atmospheric and Climate Science, ETH Zurich, Universitätstrasse 16, CH-8092 Zurich, Switzerland. (heini.wernli@env.ethz.ch)

M. Zimmer, Institute for Atmospheric Physics, University of Mainz, Becherweg 21, D-55099 Mainz, Germany.